New Journal of Physics
An Institute of Physics and Deutsche Physikalische Gesellschaft Journal

Step–step interactions and universal exponents studied via three-dimensional equilibrium crystal shapes

M Nowicki[1], **C Bombis**[1], **A Emundts**[1], **H P Bonzel**[1]† **and P Wynblatt**[2]

[1] Institut für Schichten und Grenzflächen, ISG 3 Forschungszentrum Jülich, D-52425 Jülich, Germany
[2] Carnegie-Mellon University, Department of Materials Science and Engineering, Pittsburgh, PA 15213, USA
E-mail: h.bonzel@fz-juelich.de

New Journal of Physics **4** (2002) 60.1–60.17 (http://www.njp.org/)
Received 26 April 2002, in final form 16 July 2002
Published 8 August 2002

Abstract. Equilibrated three-dimensional Pb crystallites, supported on Ru(001) and of about 1 μm diameter, were imaged by scanning tunnelling microscopy at 298–393 K. The top section of the crystallites exhibited large (111) facets and, depending on temperature, smaller (112) facets. The vicinal shapes close to (111) were analysed in detail to determine the critical shape exponent and the step–step interaction energy as well as the interaction constant of the potential. Analyzing the complete shape in sections of 1° or 3° azimuthal increments and averaging over all sections of one crystallite, we found a shape exponent of 1.490. The exponent is very close to the theoretically predicted universal value of $3/2$ and as such clear evidence for the $1/x^2$ step interaction potential. Several crystallites had dislocations threading the (111) facet. For those crystallites the step interaction energy was determined as 16 meV Å^{-2} at about 350 K, equivalent to a dipole interaction energy of 8.1 meV Å^{-2} at 0 K. The interaction constant for the dipole–dipole part of step interaction was found to be 115 meV Å.

1. Introduction

The thermodynamic equilibrium crystal shape (ECS) is dictated by the orientation dependence of the surface free energy. The latter is in general a complicated function of the surface structure,

† Author to whom any correspondence should be addressed.

1367-2630/02/000060+17$30.00

in particular of the density of steps and their mutual interactions. For surfaces vicinal to a low-index facet, the anisotropic surface free energy in one dimension, $f(p)$, is approximated by an expansion in step density, $p = \tan\theta = \mathrm{d}z/\mathrm{d}x$, where $z(x)$ is the one-dimensional (1D) shape function,

$$f(p) = f_0 + f_1 p + f_2 p^2 + f_3 p^3 + f_4 p^4 + \cdots, \tag{1}$$

f_0 is the surface free energy of the flat facet, f_1 the free energy of an isolated step, and f_2, f_3 and f_4 are step interaction energies, respectively [1]–[4]. Equation (1) is generally believed to be valid for a limited angular range of about 15° but is, in principle, capable of fitting experimental vicinal shapes at even larger angles, especially at elevated temperature and if all terms are allowed. The question is then: do all step interaction terms have a well understood physical origin? The answer is a partial yes, since unambiguous evidence for the quadratic term in step density which formally corresponds to a long-range $1/x$ step interaction potential and may physically be due to quantum effects arising from the interaction of electronic surface states with steps [5, 6] thus far is missing. In fact, the total step interaction energy for a vicinal surface calculated on the basis of a $1/x$ interaction potential would clearly diverge [7]. However, a negative f_2 has been found to describe the behaviour of a network of crossing steps on some vicinal surfaces [8, 9]. By comparison, the physical basis for step interactions of type f_3 and f_4 is well understood [2, 7, 10, 11]. Entropic interaction due to kink formation and step meandering as well as dipole–dipole interactions are characterized by $1/x^2$ potentials which are believed to be the major sources of physical step interaction. A longer-range $1/x^3$ potential has also been considered, attributable to a meaningful dipole–quadrupole interaction [7]. Because of this situation, the quadratic term in equation (1) is frequently neglected in a discussion of step interactions or in attempting to fit experimental data, with a few notable exceptions [12]–[14]. The fundamentally important question of whether hard evidence for the existence of a $f_2 p^2$ term can be identified in experimental shapes of equilibrated crystallites has not been settled.

A frequently practised procedure of checking this issue is to analyse the vicinal shape of equilibrated small three-dimensional (3D) crystallites in terms of a universal shape exponent [13, 15]–[18]. Special exponents of $3/2$ (Pokrovsky/Talapov [19]) or 2 (mean field [20]) have been discussed in context with ^{4}He, Pb, In and Si crystallites. In this paper we address this general issue again in context with new ECS data of Pb and their detailed evaluation for a number of different conditions. In the course of this investigation we are going to compare the influence of either $f_2 p^2$ or $f_4 p^4$ terms in (1), in addition to the established $f_3 p^3$ term. Particular attention is paid to any systematic dependence of shape exponents with azimuth or polar angle range [21]. The procedure is based on mathematical shape functions, obtained by Legendre transforms of the anisotropic surface free energy, with either $f_2 p^2$ or $f_4 p^4$ term included.

2. General considerations

In this section we briefly describe the methodology of evaluating the vicinal shape of faceted crystallites believed to be in their equilibrium state. Three properties shall be in the focus of this evaluation: the value of the vicinal shape exponent, the dependence of the exponent on the range of polar angle, θ (equivalent to a range of x relative to the facet radius), and the variation of the exponent with azimuthal angle, ϕ. The average value of the exponent and its possible dependence on x-range is expected to yield detailed information on the physics of step interaction, e.g. on the relative magnitude of various terms contributing to equation (1). Any

systematic variation of exponent with azimuth is suspected to indicate non-universal behaviour or simply non-equilibrium and/or improper evaluation conditions, such as an extended vicinal range which is too large for equation (1) to be valid. The latter may be clarified by an analysis of the apparent exponent versus range behaviour.

As already mentioned, the classic case of step–step interactions is clearly governed by a $1/x^2$ potential, accounted for by the third-order term in equation (1). Integration yields the following vicinal shape function [22]:

$$z(x) = \begin{cases} z_0 - \dfrac{2}{3}\left(\dfrac{\lambda}{3f_3}\right)^{1/2}(x - x_0)^{3/2}, & x \geq x_0 \\ z_0, & x < x_0 \end{cases} \tag{2}$$

where z_0 and x_0 are the coordinates of the facet boundary and λ is the Lagrange parameter. The latter is, for regular shapes, equal to the step free energy over the facet radius, f_1/r_f [22]. The shape is characterized by the universal exponent $3/2$ which is expected to be independent of facet orientation, azimuthal angle, evaluated x-range, or temperature. This case is also referred to as the Pokrovsky/Talapov facet-to-vicinal transition [19].

In general, when other terms in equation (1) contribute to step interaction, the vicinal shape function will not be as simple as equation (2) but contain additional terms. Hence the exponent will no longer be universal but will depend on the range of x and other variables. In this general case we define an apparent exponent which is evaluated from measured (or computed) shapes by fitting to the following function:

$$z(x) = \begin{cases} z_0 - A(x - x_0)^n, & x \geq x_0 \\ z_0, & x < x_0. \end{cases} \tag{3}$$

Here A is a prefactor (general measure of step interaction) and n a variable exponent. Fitting 1D shape profiles by equation (3) as a function of azimuth φ or range of x, a variable exponent $n(\varphi)$ or $n(x)$, respectively, can be obtained [21].

For these more general cases, the vicinal shape of a crystallite in relationship to the assumed orientation-dependent surface free energy is obtained also by a Legendre transform of equation (1) [20, 23]:

$$z = \frac{1}{\lambda}\left(f(p) - p\frac{\mathrm{d}f}{\mathrm{d}p}\right), \qquad x = -\frac{1}{\lambda}\frac{\mathrm{d}f}{\mathrm{d}p} \tag{4}$$

with the boundary condition $z(x_0) = z_0$ and $\mathrm{d}z/\mathrm{d}x = 0$ at $x = x_0$. Several cases are well known. Firstly, with both the third- and fourth-order step interaction terms included in equation (1), the solution is [22]

$$z(x) = \begin{cases} z_0 - \dfrac{2}{3}\left(\dfrac{\lambda}{3f_3}\right)^{1/2}(x - x_0)^{3/2} + \dfrac{\lambda f_4}{3f_3^2}(x - x_0)^2 + \cdots, & x \geq x_0 \\ z_0, \quad x < x_0. \end{cases} \tag{5}$$

In this case the exponent is expected to vary from $3/2$ for a small range of x (i.e. close to the facet) to 2 for a large range of x. The exponent is expected to be independent of azimuth.

Secondly, when instead of the fourth order the second-order term is included in equation (1), the solution, containing now a term linear in x, is as follows [12, 13]:

$$z(x) - z_0 = \frac{2f_2^3}{27\lambda f_3^2} + \frac{f_2}{3f_3}(x - x_0) - \frac{2}{3}\left(\frac{\lambda}{3f_3}\right)^{1/2}\left(x - x_0 + \frac{f_2^2}{3\lambda f_3}\right)^{3/2}, \qquad x \geq x_0$$
$$z(x) = z_0, \qquad x < x_0. \tag{6}$$

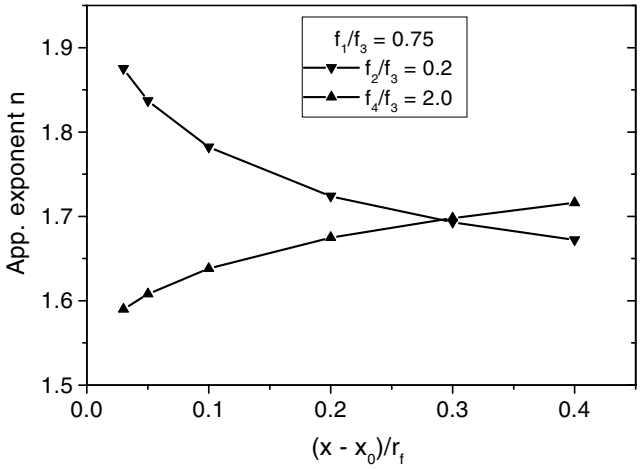

Figure 1. Plot of the apparent shape exponent n versus range $(x - x_0)/r_f$ for the two cases of long-range interaction $f_2/f_3 = 0.2$ and short-range interaction $f_4/f_3 = 2.0$, respectively, with a fixed $f_1/f_3 = 0.75$.

Here the apparent exponent drops from near 2 at small x towards $3/2$ with increasing range of x. The general behaviour for the two cases, equations (5) and (6), is illustrated in figure 1 for an arbitrary set of energy ratios. The length scale of the abscissa is expressed as x/r_f, where r_f is the local facet radius. The facet edge is for simplicity located at $x = 0$ (i.e. $x_0 = 0$). The opposite functional behaviour of $n(x/r_f)$ with a crossover at $x/r_f = 0.3$ provides a clear signature for distinguishing a dominant long- or short-range additional step interaction term. If shape exponents can be accurately obtained from measured ECS over a sufficiently large vicinal range, the tendency in x/r_f should clearly indicate the kind of additional step interaction. On the other hand, if neither of the additional step interaction terms is important, average exponents should be close to $3/2$ and independent of azimuth and range of x.

In an attempt to prepare for a comparison of theoretical and experimental data, we define energy ratios and calculate $n(x/r_f)$ for the two cases defined by equations (5) and (6) for a larger set of parameters. It is noteworthy that both shape functions depend on only two independent variables. These are f_1/f_3 and f_4/f_3 in equation (5) and f_2/f_3 and f_1/f_3 in equation (6). At this point our aim is to first choose a reasonable value of f_1/f_3 and then check how large the influence of an added f_2/f_3 or f_4/f_3 on vicinal shapes and apparent exponents is going to be. For this reason we consider some reasonable boundary conditions of the problem.

As we have seen from the shape functions above, it is most important to determine the apparent exponent close to the facet edge, to decide whether long-range f_2 or short-range f_4 step interactions are important. Let us assume that we restrict this range to 30% of the facet radius, i.e. the vicinal shape is evaluated to a maximum of $x/r_f = 0.3$. Furthermore, the expression for $f(\theta)$ is considered to be valid for small angles, e.g. $\theta < 15°$. If we now calculate the maximum slope as a function of f_1/f_3, for the shape functions of equations (2), (5) and (6), we find limiting values of f_1/f_3 for which the conditions of maximum range and slope are fulfilled. The result of such a calculation is shown in figure 2(a). For the Pokrovsky/Talapov shape f_1/f_3 should be smaller than 0.75, while an additional short-range interaction, $f_4/f_3 = 0.2$, reduces the limit to 0.5. By comparison, an additional long-range interaction, $f_2/f_3 = 0.4$, increases the limit to

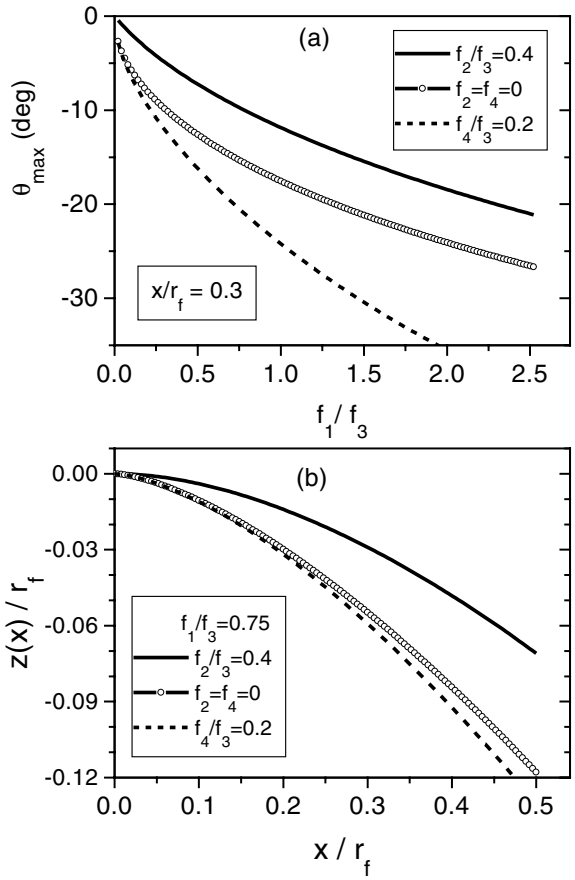

Figure 2. (a) Plot of maximum polar angle (relative to the (111) facet) versus f_1/f_3 ratio, with either a finite long-range step interaction $f_2/f_3 = 0.4$, no additional interaction $(f_2/f_3 = 0)$, or an added short-range step interaction $f_4/f_3 = 0.2$. (b) Corresponding dependence of profile shape $z(x)/r_f$ versus x/r_f, with a fixed $f_1/f_3 = 0.75$. Other conditions as in (a).

$f_1/f_3 < 1.5$. This behaviour demonstrates also that fitting vicinal shapes with either equation (5) or (6) will lead to low or rather high values of f_1/f_3, respectively. The actual shapes calculated with the mentioned parameter sets are illustrated in figure 2(b).

In the following we analyse the dependence of the apparent shape exponent on the evaluated vicinal range for a set of parameters f_4/f_3 and f_2/f_3, assuming a fixed value of $f_1/f_3 = 0.75$. The relative strength f_4/f_3 was varied between 5.0 and 0.4. Apparent exponents were determined for a range of $x/r_f = 0.05$–0.4, with the results summarized in figure 3(a). There is a strong increase in n for small x/r_f, especially visible for strong f_4 interaction. At $x/r_f > 0.1$ n rises more slowly, with its change being proportional to f_4/f_3.

In the second case, equation (6), we note that this equation can be rewritten in the following simple form:

$$\frac{z(x)}{r_f} = C\left\{D + \frac{3x}{2r_f} - D^{-1/2}\left(\frac{x}{r_f} + D\right)^{3/2}\right\}, \qquad x > 0 \tag{7}$$

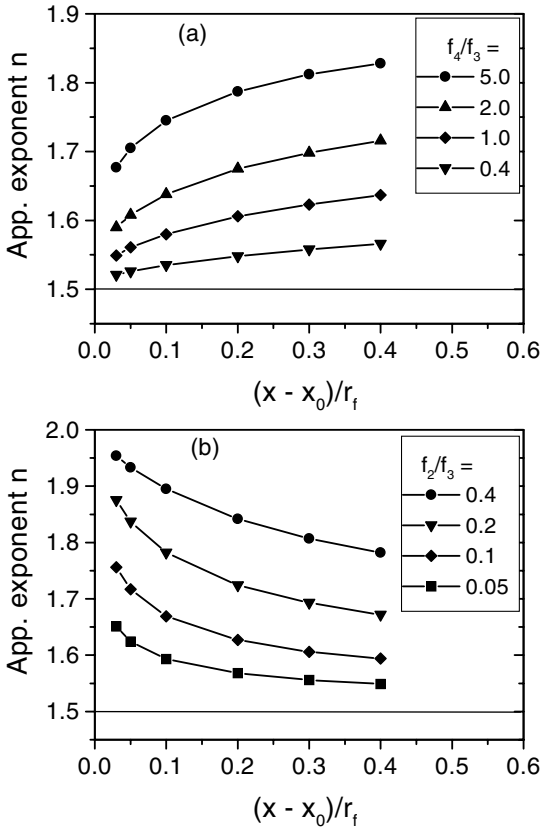

Figure 3. Characteristic dependence of apparent shape exponent on kind of added step interaction. (a) Added short-range step interaction f_4/f_3 causing an increase of n with $(x - x_0)/r_f$. (b) Added long-range step interaction f_2/f_3 causing a decrease of n with $(x - x_0)/r_f$.

with $C = 2f_2/9f_3$ and $D = f_2^2/3f_1f_3$. Again, f_1/f_3 is kept fixed at 0.75 and f_2/f_3 is varied between 0.05 and 0.4. The apparent exponent versus x/r_f is shown in figure 3(b). Analogous to figure 1, now n decreases with increasing x/r_f whereby the changes in values of n are roughly proportional to f_2/f_3. Overall, the long-range interaction energy f_2 has a much stronger influence on the apparent exponent than the short-range energy f_4.

At this stage we mention that the choice of $f_1/f_3 = 0.75$ based on our estimate does not agree well with previous experiments where a ratio of about 2.4 has been reported [12, 13]. However, in both studies a second-order term f_2p^2 has been assumed in the evaluation of Pb(111) and In(111) vicinal surfaces. As we can see from figure 2(a), when shapes are fitted by equation (6) with a finite value of f_2/f_3, the initial slopes are much smaller and the limit of 15° is reached at a much higher f_1/f_3. Alternatively, recent measurements of the Pb ECS have been found to correspond to ideal Pokrovsky/Talapov shapes, equation (2), where the shape exponent was determined over all azimuths, in increments of 2°, and its average came out to be close to 1.5 [24]–[26]. For these crystallites, absolute step free energies for Pb(111) vicinal surface have been determined and the step interaction energy has been estimated. With the average value of $f_1 = 12.4$ meV Å^{-2} (at $T = 0$ K) [27] and $f_3 = 47$ meV Å^{-2} [24] we have $f_1/f_3 = 0.26$, a ratio which is significantly smaller than the limit discussed above. Here the

evaluated angular vicinal range was quite small. A related case is the investigation of Si shapes equilibrated at 900 °C [18]. Vicinal shapes in high-symmetry azimuths could be well fitted by equation (2) over an angular range of 3°–17° (relative to Si(111)). The interaction energy f_3 was determined to be 44.4 meV Å^{-2} and the ratio f_1/f_3 came out to be 0.17, which is again typical in the absence of any long-range f_2 step interaction energy. On the other hand, the initial vicinal range between 0° and 3° could not be fitted by equation (2), giving rise to new speculations about a long-range step interaction law [18]. Data for Pb will be presented in the following section to substantiate the earlier results on the universal exponent $3/2$ and the step interaction energy.

3. Experimental shapes and exponents

In this section we report new quantitative data on the ECS of Pb crystallites annealed at 300–400 K and imaged by scanning tunnelling microscopy (STM). Crystallites were annealed at least 70 h prior to recording first images at the annealing temperature. Further experimental details have been published previously [21, 24, 26]–[30]. All of the Pb crystallites show a threefold symmetric (111) facet parallel to the substrate surface. This facet and its complete range of vicinal surfaces, i.e. for an azimuthal range of 360° and a polar range of up to 18° (relative to the facet at 0°), are subject of investigation. An automatic evaluation routine seeks the facet boundary and the facet's centrepoint. Line profiles through the centre are created at all azimuths (typically in increments of 1°–3°) which are then fitted by equation (3) to obtain apparent exponent n and prefactor A. The resulting n and A are plotted versus azimuth ϕ and, in the absence of any systematic variation of $n(\phi)$ and $A(\phi)$, average values of $\bar{n}$ and $\bar{A}$ are determined. When a small azimuthal section of strongly diverging numbers $n(\phi)$ and $A(\phi)$ is found, they are discarded from the averaging data set. In each case a continuous azimuthal section of at least 280°–360° enters the evaluation.

Figures 4(a) and (b) show images of a Pb crystallite, total and close-up of (111) facet and vicinal range, annealed at 298 K. The facet in this case exhibits a single step emerging at a dislocation endpoint. STM images of another crystallite annealed at 393 K are presented in figures 4(c) and (d). Here the (111) facet (without dislocation) is smaller and less anisotropic than for the 298 K crystallite, a clear effect of the increased temperature [27, 30]. The corresponding plots of the azimuth-dependent $n(\phi)$ and $A(\phi)$ for both crystallites are shown in figures 5 and 6, respectively. There is considerable scatter in both $n(\phi)$ and $A(\phi)$ which shows that a single line profile can never provide a reliable answer to the shape exponent and step interaction energy. The main reason for the scatter is noise in the image, caused by Pb-specific surface-to-tip contacts [31]. The average values of $\bar{n}$ and $\bar{A}$ for the two cases are 1.470 and 0.0175 nm$^{-1/2}$ and 1.487 and 0.011 nm$^{-1/2}$, respectively. Several additional crystallites of different sizes, annealed at different temperatures, were evaluated for $x/r_f \leq 0.3$. All of the results are listed in table 1. The average exponents are in each case close to 1.5 and do not show a significant trend with the evaluated range x/r_f, such as seen in figure 7 for two crystallites. Hence there is no necessity to assume an additional step interaction term in the sense of section 2. The overall average (from all studies) of the exponent $\bar{n}$ is equal to 1.490, in excellent agreement with equation (2) and in full support of a dominant $1/x^2$ step interaction potential for Pb.

When the equilibration temperature is below 325 K and the range of evaluation exceeds about $x/r_f = 0.5$, some well developed small facets, such as (112), can be recognized in the images. These facets are included in the range of fitting, leading to a threefold symmetric

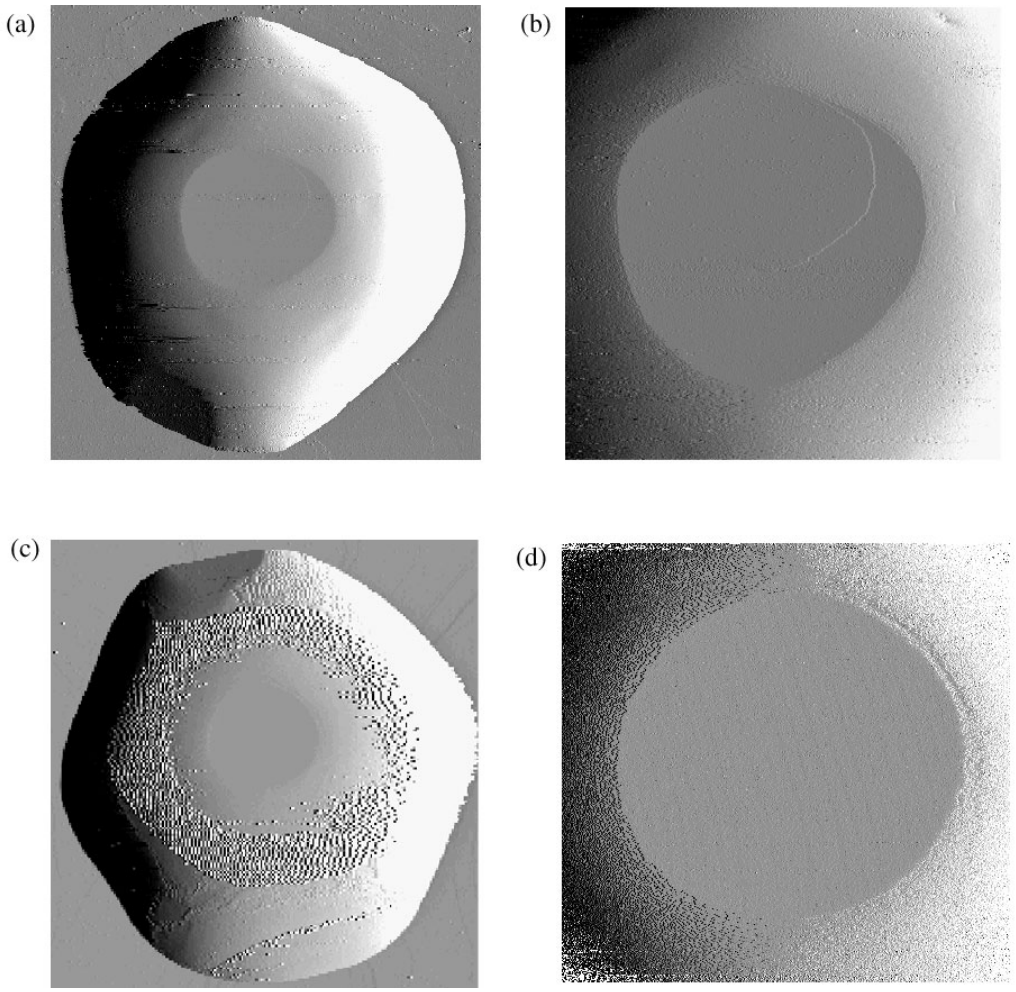

Figure 4. STM images of equilibrated crystallites and close-ups of their main (111) facets and vicinal surface. (a) Crystallite annealed and imaged at 298 K, with (111) facet in the centre and small (112) as well as (110) facets visible; image size: $1070\ \mathrm{nm} \times 1015$ nm. (b) Section of crystallite in (a) showing (111) facet with a single dislocation emerging near the centre. Image size: $550\ \mathrm{nm} \times 570$ nm. (c) Crystallite annealed and imaged at 393 K, image size: $1235\ \mathrm{nm} \times 1180$ nm. Note the circular band of tip-induced roughness around the (111) facet, caused by tip-to-surface contacts, typical for this elevated temperature. (d) Section of crystallite shown in (c) with the (111) facet. Image size: $450\ \mathrm{nm} \times 440$ nm.

variation in $n(\phi)$ and $A(\phi)$. Since the (112) type facets (at 19.5° relative to (111)) are part of the line profiles in the direction of A-steps, they cause large apparent n and low prefactors A in these particular azimuths. An example for this behaviour is presented in figure 8 for a range of $x/r_f = 0.9$. Note also that the noise is much reduced compared to figures 5 and 6 because for each line scan the data base is larger by a factor of three. The oscillatory effect of $n(\phi)$ and $A(\phi)$ had been seen before and was at the time prematurely attributed to non-universal behaviour or poorly equilibrated crystallites [21, 32]. The correct interpretation of this effect rests now on the recognition of the (112) facets but also on investigating the change in apparent exponents with

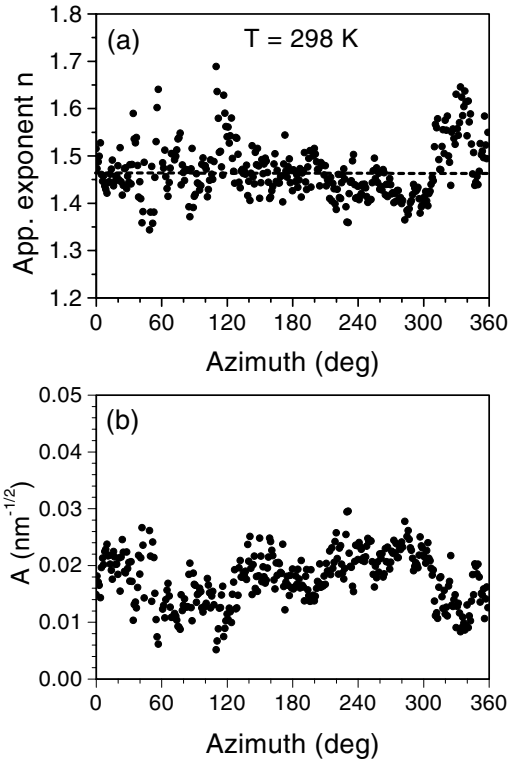

Figure 5. Evaluated data of Pb crystallite annealed at 298 K. (a) Apparent exponent n versus azimuth; average value of 1.470. (b) Prefactor A, equation (3), versus azimuth, with average value of 0.0175 $\mathrm{nm}^{-1/2}$.

Table 1. Average values of $\bar{n}$ and $\bar{A}$ and of the step interaction energy $f_3(T)$ evaluated from detail images of (111) facets and limited vicinal range (except Cr). The vicinal x-range included in the evaluation was in all cases equal or smaller than $x/r_f = 0.3$, corresponding to a maximum polar angle of $<12°$ (D = dislocation visible in (111) facet; Cr = total crystallite image).

Crystal	T_{ann} (K)	r_f (nm)	θ_{max} (deg)	$\bar{n}$	$\bar{A}$ ($\mathrm{nm}^{-1/2}$)	$(r_f\bar{A}^2)^{-1}$	f_1 [27] (meV Å^{-2})	f_3 (meV Å^{-2})
m1182D[a]	298	187	12	1.484	0.0251	8.49	10.67	13
m1193	298	163	10	1.470	0.0175	20.03	10.67	32
m235D[a]	308	284	12	1.504	0.0194	9.36	10.56	15
m447	323	133	11	1.493	0.0173	25.12	10.40	39
m369	353	188	12	1.502	0.0182	16.05	10.03	24
m413D, Cr	373	155	11	1.507	0.0247	10.57	9.78	15
m231[b]	383	270	9	1.487	0.0110	30.58	9.67	44
m1108	393	168	10	1.458	0.0167	21.32	9.53	30
m839D,Cr[a]	393	125	14	1.508	0.0241	13.80	9.53	20
Average:				1.490			10.09	See text

[a] 0–270° azimuthal range evaluated.

[b] Crystallite image provided by Konrad Thürmer of the Physics Department, University of Maryland.

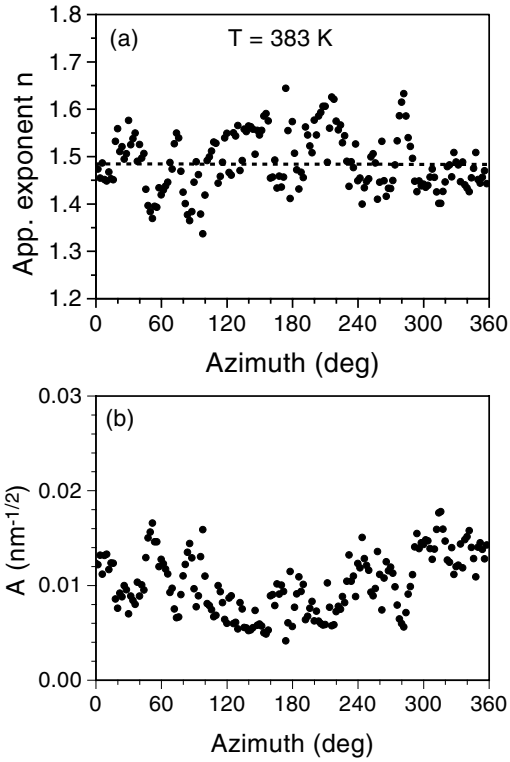

Figure 6. Evaluated data of Pb crystallite annealed at 383 K. (a) Apparent exponent n versus azimuth; average value of 1.487. (b) Prefactor A, equation (3), versus azimuth, with average value of 0.0110 $\mathrm{nm}^{-1/2}$.

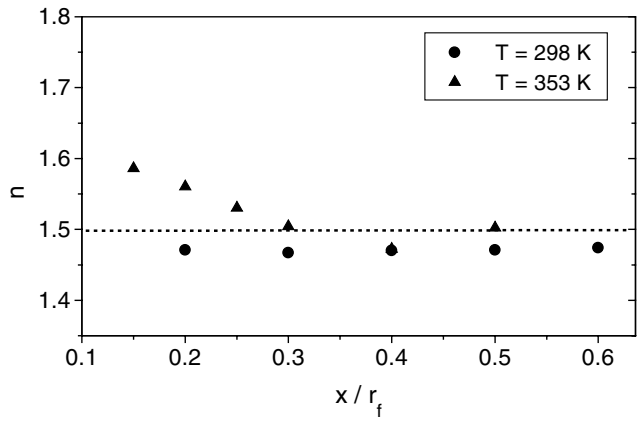

Figure 7. Plot of apparent shape exponent versus x/r_f for two crystallites, annealed at 298 and 353 K, respectively.

increasing evaluated range x/r_f. A corresponding re-evaluation of the older data was carried out and supported the current interpretation.

Aside from the cases listed in table 1 and the mentioned periodic variation of $n(\phi)$ and $A(\phi)$ for large x/r_f, we observed also crystallites where $\bar{n}$ and $\bar{A}$ deviated significantly from the Pokrovsky/Talapov universal value of $3/2$ in the range $x/r_f \leq 0.3$. These crystallites exhibited

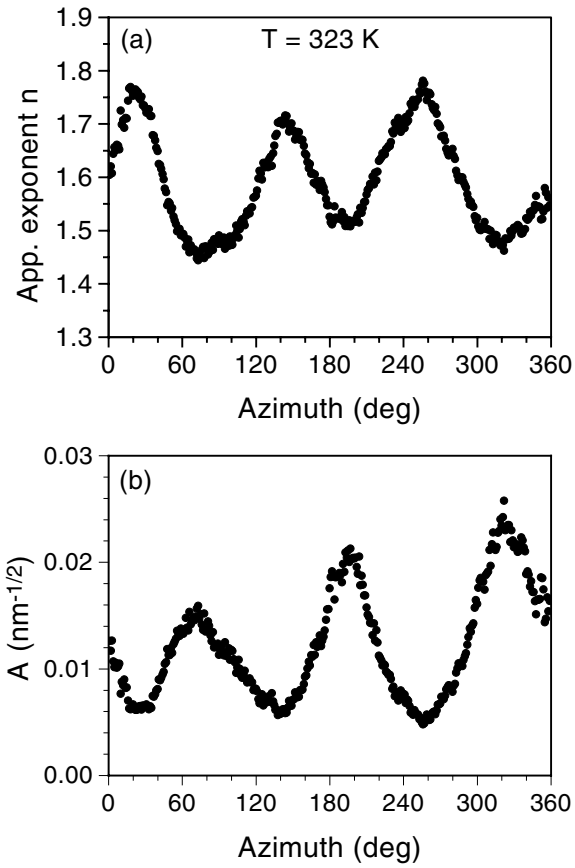

Figure 8. Evaluated data of Pb crystallite annealed at 323 K. Here the evaluation has been carried out for a larger range up to $x/r_f = 0.9$. (a) The apparent exponent n versus azimuth shows a strong variation, with maxima in the direction of A-steps and minima in the direction of B-steps. The average exponent is 1.59. (b) Prefactor A, equation (3), versus azimuth shows a similar systematic dependence as the exponent.

Table 2. Average values of $\bar{n}$ and $\bar{A}$ for apparently non-equilibrated or contaminated crystallites. The vicinal range x/r_f evaluated was equal or smaller than 0.3.

Crystal	T_{ann}/T_{meas} (K)	r_f (nm)	$\bar{n}$	$\bar{A}$ (nm$^{-1/2}$)
m567	413	116	1.149	0.0587
m900	323	68	1.196	0.0591
m988	450/120	190	1.84	0.009

unusually small facets and their evaluation yielded apparent exponents of about 1.2 and prefactors of 0.06 nm$^{-1/2}$ (see table 2). Since we do not know an appropriate physical model to explain such low exponents, we believe that the corresponding crystallites are in a non-equilibrium state, possibly due to surface impurities of unknown origin [30].

Another unusual case was a crystal which had been annealed at 450 K and then quenched to 120 K by liquid nitrogen cooling to preserve the shape achieved at high temperature. The low temperature brought about an improvement in STM imaging because image degrading tip-to-surface contacts were found to be nearly absent at temperatures below 320 K. However, an important disadvantage is here that the actual cooling rate of the sample stage and crystallite is not known. Therefore it is questionable whether a truly equilibrated state is frozen in by this procedure. The evaluation of this crystallite produced an average exponent of $\bar{n} = 1.84$ and $\bar{A} = 0.009$, with no systematic azimuthal variation nor a clear $n(x/r_f)$ dependence in the sense of figure 1. The (111) facets are large and their shape is typical of a higher temperature but the high average value of the exponent seems to indicate a non-equilibrated vicinal shape.

4. Step–step interaction energy

In the unique case where the crystallite is in thermodynamic equilibrium and the vicinal shape is described by equation (2), with the average shape exponent being close to the universal value of $3/2$, the step interaction energy is well defined and readily available from the prefactor A averaged over all azimuths. The relationship is as follows:

$$f_3(T) = \frac{4 f_1(T)}{27 \bar{A}^2 r_f} \tag{8}$$

$\bar{A}^2$ is in units of inverse length (nm^{-1}), r_f in (nm), such that f_3 has the same units as f_1. Although the (111) facet is anisotropic under equilibrium conditions, the ratio $\lambda = f_1/r_f$ is equal to the chemical potential and therefore constant. Hence we take values of r_f from experiment and of f_1, at the temperature of equilibration, from [27], both quantities averaged over A- and B-steps. Of course, the prefactor A is allowed to vary with the nature of steps. For a fcc(111) vicinal surface there are structurally inequivalent A- and B-steps for which a different value of A may be expected. However, this was not observed experimentally (see figures 5–6). Using the relation $\lambda = f_1/r_f$ requires the crystallite to be in full 3D thermodynamic equilibrium. Since the growth (or shrinkage) of facets to their equilibrium diameter may be hindered by an activation barrier [33]–[35], at least for isolated 3D crystallites, the issue of having reached the equilibrium state is critical for the evaluation of the step interaction energy. A reliable value can only be expected if full equilibration can be ascertained. However, this is in principle a difficult task, unless it can be shown that the conditions for the existence of an activation barrier are not applicable. This is the case if evaporation or other forms of material exchange with the environment may occur, or if dislocations emerge in the area of facets. While evaporation of Pb at the temperatures of investigation is negligible and the degree of diffusional exchange is unknown, we found that single dislocations were indeed visible in several of the (111) facets imaged by STM. An example is shown in figure 4(b). Thus we classify the results obtained into two categories, one for crystals with non-dislocated facets and the other with dislocated facets, the latter being definitely characteristic of fully equilibrated crystallites. This is at least true in the vicinity of these facets while other facets of the same orientation on the same crystallite may exhibit different diameters because they may not contain a dislocation. This issue may be worth being checked in future studies where possible.

As seen in table 1, the formal evaluation of the total step interaction energy f_3 for all vicinal shapes, where the average exponent is near $3/2$, yields a considerable spread of values between 13 and 44 meV $\mathrm{Å}^{-2}$. This large variation is not likely to be due to STM imaging problems.

The classification of crystallites mentioned above helps to understand the origin of the large spread in numbers. Those crystallites where the (111) facet exhibits a dislocation emerging in its area yielded step interaction energies in the range of 13–20 meV Å^{-2}, while those with no dislocations yielded 24–44 meV Å^{-2}. Averaging over the values in each category results in f_3 of about 16 meV Å^{-2} for crystallites with dislocated facets and 34 meV Å^{-2} for all others. A small increase of f_3 with temperature in the range 300–400 K can be noticed for each category. Based on the assumption that only crystallites with dislocated facets are likely to be equilibrated, we conclude that $f_3 = 16$ meV Å^{-2} is a reliable value of the total step interaction energy at these elevated temperatures.

Why is the apparent f_3 for non-equilibrated crystallites larger than for equilibrated ones? Assuming that the facet does not reach its full equilibrium diameter leaves more room for the vicinal steps to expand. Calculating the separation between the first and second step, $x_0 - x_1$, for example, as a measure of spreading (first step is the facet edge) by using equation (2) we find

$$x_0 - x_1 = [(27/4)\, h^2 z_0 f_3 / f_0]^{1/3} \tag{9}$$

where z_0 is the separation between the facet and the centre of the crystallite. Comparing the cases 'equilibrium' and 'non-equilibrium' yields the relationship

$$\frac{(x_0 - x_1)_e^3}{(x_0 - x_1)_{ne}^3} = \frac{f_{3e}}{f_{3ne}}. \tag{10}$$

We have assumed z_0 to be constant. Based on the evaluated ratio $f_{3e}/f_{3ne} = 0.47$ we find that the equilibrium separation between the first and second step is only 78% of that in the non-equilibrium case, indicative of the facets without dislocation being too small. Hence incompletely developed facets lead to a vicinal surface whose evaluation in terms of equation (2) leads to a step interaction energy too large compared to its equilibrium value.

Equation (8) can also be used to obtain the ratio $f_1/f_3 = 6.75 r_f \bar{A}^2$. This value is independent of any predetermined energies and can be compared with our estimate given above in connection with figure 2(a). We find that the experimental f_1/f_3 is close to 0.63 and similar to that found for Si(111) vicinal shapes [18] both of which are not far from the estimate of 0.75 but well below previously reported energy ratios for Pb and In vicinal surfaces [13, 36].

The new estimate of an absolute step interaction energy $f_3(T)$ can be analysed in the frame of step–step interaction physics. The theoretical dependence of $f_3(T)$, including the entropic part of step interaction, f_{3e}, and the part due to dipole–dipole interaction, accounted for by a fitting parameter A_{dd} [37, 38], is as follows:

$$f_3(T) = \frac{f_{3e}(T)}{4}\left\{1 + \left(1 + \frac{4A_{dd} h \tilde{f}_1(T)}{(kT)^2}\right)^{1/2}\right\}^2 \tag{11}$$

where h is the height of a monatomic step. The part due to dipole–dipole interaction is given by $f_3(0) = \pi^2 A_{dd}/6h^3$ where A_{dd} is the proportionality constant in the $1/x^2$ step interaction potential. This constant is in units of meV Å if $f_3(T)$ and the step stiffness $\tilde{f}_1(T)$ are in units of meV Å^{-2}. The entropic step interaction and step stiffness are given by [39, 40]

$$f_{3e}(T) = \frac{\pi^2 (kT)^2}{6h^4 \tilde{f}_1(T)}, \qquad \text{with } \tilde{f}_1(T) = \frac{2kT}{3hd}\left\{\exp\left(\frac{\varepsilon}{kT}\right) - 4\exp\left(-\frac{2\varepsilon}{kT}\right)\right\} - TS_{vib} \tag{12}$$

where ε is the formation energy of kinks, d the nearest neighbour separation (parallel to the step), and TS_{vib} the vibrational entropy contribution of steps, chosen to be 0.0032 meV (K Å^2)$^{-1}$ [27, 41]. Both functions $f_3(T)$ and $f_{3e}(T)$ are shown in figure 9(a). The entropic part is calculated with

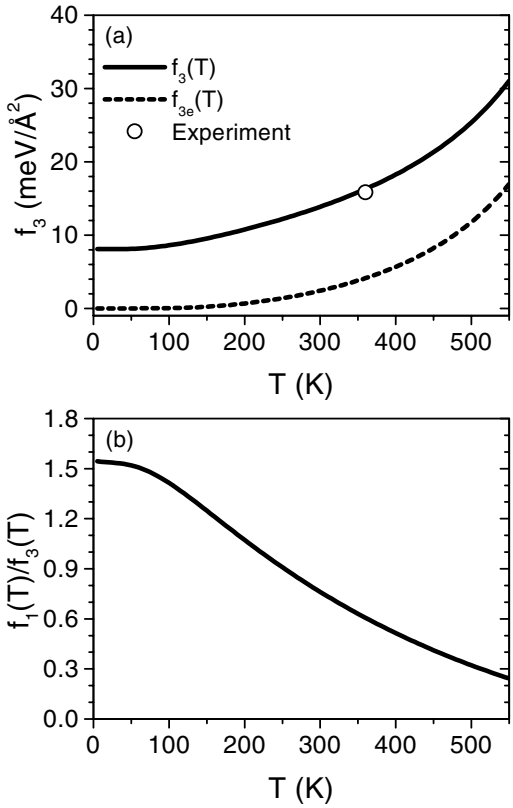

Figure 9. (a) Plot of temperature-dependent step interaction energies $f_3(T)$ and $f_{3e}(T)$, according to equations (9) and (10), respectively. A value of $A_{dd} = 220$ meV Å is chosen to fit equation (11) to the experimental best value of $f_3 = 25.4$ meV Å^{-2} at a mean $T = 350$ K. (b) Based on the available data, the function $f_1(T)/f_3(T)$ versus T is calculated. Its values are well below one for all T, in agreement with the estimate (see text).

a kink energy of 40 meV/atom for A-steps [27]. Despite the low kink formation energy, $f_{3e}(T)$ is a relatively small portion of the total step interaction (at low T) based on fitting equation (11) to the single experimental f_3 value (average over four equilibrated crystallites, facets with dislocations in table 1) at the mean temperature of 350 K. This process yields $A_{dd} = 115$ meV Å and a pure dipole interaction energy $f_3(0) = 8.1$ meV Å^{-2}. The values fall right into the range obtained by Najafabadi and Srolovitz [7] who calculated the elastic step interaction energies on vicinal surfaces of various fcc metals. They find a range of 5.3–43.2 meV Å^{-2} for f_3, equivalent to A_{dd} ranging from 42 meV Å (Ag) to 304 meV Å (Pt). We can also estimate A_{dd} (Pb) via the Marchenko and Parshin relation to the surface stress of Pb(111) [11]. Using a theoretical surface stress of 51 meV Å^{-2} reported by Mansfield and Needs [42], we obtain $A_{dd}\,(\mathrm{Pb}) = 155$ meV Å. This compares well to our experimental value of 115 meV Å considering that the formula due to Marchenko and Parshin generally overestimates the step interaction energy [43].

In this context it is also of interest to calculate the ratio of step-to-step interaction energy, f_1/f_3, using the expression for the temperature-dependent $f_1(T)$ [27]:

$$f_1(T) = \frac{1}{hd}\left[f_1(0) - kT\left\{2\exp\left(-\frac{\varepsilon}{kT}\right) - \exp\left(-\frac{2\varepsilon}{kT}\right)\right\}\right] - TS_{vib}. \qquad (13)$$

The ratio $f_1(T)/f_3(T)$ depends now on step energy at 0 K, step stiffness and the interaction constant A_{dd} of dipole–dipole interaction. Its temperature dependence in figure 9(b) illustrates that this ratio is consistent with our previous estimate.

Now we turn to cases where the average exponent deviates from $3/2$. When $n > 1.5$, such as in figure 3, at least two step interaction terms in equation (1) will be responsible for this, leading to shape equations (5) and (6). If the dependence $n(x/r_f)$ is known experimentally, individual fitting of vicinal shapes to either equation (5) or (6) will yield estimates of the energy ratios f_1/f_3 and f_4/f_3 or f_2/f_3 and f_2/f_1, respectively. Finally, if the apparent exponent is <1.5, no meaningful evaluation of the step interaction energy can be carried out at the present time because no theoretical model or relationship exists which explains such low exponents. In fact, crystallite shapes characterized by such low apparent exponents may not be in thermodynamic equilibrium, possibly due to a reduced surface diffusion rate and step pinning, caused by a partial coverage with a contaminant, for example.

5. Discussion

The present investigation of ECS of Pb shows for the first time that the vicinal shape exponent, averaged over a 360° azimuthal range, is very close to the universal value of 1.5. Hence the facet-to-vicinal transition for Pb(111) is of the Pokrovsky–Talapov type [19, 44]. This experimental result is therefore in perfect agreement with theories of step–step interaction due to kink formation and step meandering (entropic interaction) [10] and dipoles (elastic as well as electrostatic) [11, 22]. It follows that the corresponding $1/x^2$-interaction potential of monatomic steps is dominant in this case and maybe for metals in general. A comparable experimental result had been obtained for Si crystals equilibrated at 1173 K but analysed only for the $\langle 110 \rangle$ azimuthal zone [18]. A polar angle range between 3° and 17° was characterized by an exponent of 1.5 but a small range next to the (111) facet exhibited serious deviations, suggested to originate from step reconstruction, from the universal value [18].

Previous reports of shape exponents near 1.6 [15, 16] or periodically varying with azimuth [21, 32] must be questioned. In the case of Pb a large angular vicinal range of 18° relative to a (111) facet had been analysed with the result that the apparent shape exponent varied from 1.88 close to the facet to 1.61 far away from the facet, with a minimum at 1.53 [15]. This behaviour indeed, as seen in figure 3(b), suggests a long-range $1/x$ step interaction in addition to the regular $1/x^2$-interaction potential which in fact led to later work where the same data were fitted by equation (6) [36]. Similar work followed for equilibrated In crystals [13] where the range of evaluation, in our terminology, was as large as $x/r_f = 2$ (corresponding to 15° polar angle). Again, a range-dependent apparent exponent from 2 to below 1.6 was found. Only very limited azimuthal information was given [13]. Another study worthy of mention, where four different ^{4}He crystals and a total of 13 vicinal profiles have been analysed, is by Carmi *et al* [16]. They reported an average exponent of $n = 1.55 \pm 0.06$ for a reasonable polar angular range up to 5.7°, in full support of the $1/x^2$ step interaction potential and in good agreement with our results for Pb.

The current results still go far beyond previous investigations. They were obtained by an extensive evaluation of high-resolution STM images of many crystallites of different sizes and annealed at different temperatures. A detailed study of vicinal shape exponents versus azimuth and also versus x-range (or polar angle of orientation) showed that $n(\phi)$ and $n(x)$ did not vary in any systematic fashion, as long as the range x/r_f did not exceed about 0.3. Averaging of

all data yielded very reasonable results, in full support of the known step interaction physics. Physical limits of a finite polar angle for a physically meaningful evaluation were found. Hence it was essential to limit the angular range of shape fitting [17] and to study the dependence of $\bar{n}$ and $\bar{A}$ versus range. We conclude that large polar angle profiles are scientifically unreasonable in this context, especially at low temperature, where extra facets can exist in the vicinity of the main facet whose vicinal range is studied. We have shown that a transition from an azimuth independent $\bar{n}$ and $\bar{A}$ to a systematically varying $n(\phi)$ and $A(\phi)$ exists when shapes are evaluated for an increasingly large vicinal range (figure 8). The fact that the exponent n seems to decrease from about 1.58 to 1.5 for increasing x/r_f in figure 7 may still be indicative of a small f_2 contribution of about $f_2/f_3 = 0.03$ (figure 3(b)) but this is nearly two orders of magnitude smaller than previously reported [13, 36].

The current study has also shown that crystallites can be distinguished as to their degree of equilibration. Those crystallites with dislocations emerging in one of the (111) facets must be fully equilibrated in the vicinity of that facet. Hence, energetic data derived from a quantitative shape analysis are expected to yield trustworthy results. In this sense we believe that the present step interaction constant $A_{dd} = 115$ meV Å and the (total) step interaction free energy $f_3 = 16$ meV Å^{-2} (the latter at about 350 K) are reliable data. At 0 K we have $f_3(0) = \pi^2 A_{dd}/6h^3 = 8.1$ meV Å^{-2} which is equal to the dipole–dipole interaction part only. In a related study of monatomic layer peeling events on (111) facets of Pb crystallites Thürmer *et al* estimate $f_3 = 6.5$ meV Å^{-2} at $T = 368$ K for a fully equilibrated crystallite [45]. This value appears to be low compared to the present data (see also figure 9). In their work they correct for the effect of an activation barrier for facet growth by a detailed discussion of single step energetics. In the same framework they also point out that step interaction energies evaluated for non-equilibrated vicinal shapes are expected to be higher than the true value representing the ECS. Since the facet stops growing (shrinking) due to the activation barrier, the force balance between the facet and the vicinal step train is shifted in favour of the latter yielding apparent step interaction energies that are too large [45]. Their approach explains the value of $f_3 = 34$ meV Å^{-2} which was formally evaluated above for crystallites with non-dislocated facets. This large value supports the suspicion that the (111) facets of those crystallites have not reached their equilibrium diameter.

Acknowledgments

We would like to thank Udo Linke for excellent preparations of the Ru(001) crystal and Peter Coenen for expert technical help. We are also grateful to Konrad Thürmer (University of Maryland) for communicating his results on Pb crystallites. Arndt Emundts thanks the DAAD and Professor Ellen Williams for supporting his research period at the University of Maryland. Paul Wynblatt wishes to acknowledge generous support by the Alexander von Humboldt Foundation and by the National Science Foundation (Grant DMR9820169).

References

[1] Cabrera N 1964 *Surf. Sci.* **2** 320
[2] Jayaprakash C, Rottman C and Saam W F 1984 *Phys. Rev.* B **30** 6549
[3] Leamy H J, Gilmer G H and Jackson K A 1975 *Surface Physics of Materials* vol 1, ed J M Blakely (New York: Academic) pp 144–8
[4] Cabrera N and Garcia N 1982 *Phys. Rev.* B **25** 6057

[5] Garcia N and Serena P A 1995 *Surf. Sci.* **330** L665
[6] Carlon E 1996 *Doctoral Thesis* University of Utrecht
[7] Najafabadi R and Srolovitz D 1994 *Surf. Sci.* **317** 221
[8] Carlon E and van Beijeren H 1996 *Phys. Rev. Lett.* **76** 4191
[9] Carlon E and van Beijeren H 2000 *Phys. Rev.* E **62** 7646
[10] Gruber E F and Mullins W W 1967 *J. Phys. Chem. Solids* **28** 875
[11] Marchenko V I and Parshin A Y 1980 *Zh. Eksp. Teor. Fiz.* **79** 257
[12] Sáenz J J and García N 1985 *Surf. Sci.* **155** 24
[13] Métois J J and Heyraud J C 1987 *Surf. Sci.* **180** 647
[14] Wang Z and Wynblatt P 1998 *Surf. Sci.* **398** 259
[15] Rottman C, Wortis M, Heyraud J C and Métois J J 1984 *Phys. Rev. Lett.* **52** 1009
[16] Carmi Y, Lipson S G and Polturak E 1987 *Phys. Rev.* B **36** 1894
[17] Balibar S, Guthmann C and Rolley E 1993 *Surf. Sci.* **283** 290
[18] Bermond J M, Métois J J, Heyraud J C and Floret F 1998 *Surf. Sci.* **416** 430
[19] Pokrovsky V L and Talapov A L 1979 *Phys. Rev. Lett.* **42** 65
[20] Andreev A F 1981 *Zh. Eksp. Teor. Fiz.* **80** 2042
[21] Arenhold K, Surnev S, Coenen P, Bonzel H P and Wynblatt P 1998 *Surf. Sci.* **417** L1160
[22] Jayaprakash C and Saam W F 1984 *Phys. Rev.* B **30** 3916
[23] Landau L D and Lifshitz E M 1958 *Statistical Physics* vol 5 (Reading, MA: Addison-Wesley) p 460
[24] Emundts A, Bonzel H P, Wynblatt P, Thürmer K, Reutt-Robey J and Williams E D 2001 *Surf. Sci.* **481** 13
[25] Bonzel H P 2001 *Prog. Surf. Sci.* **67** 45–58
[26] Emundts A 2001 Morphologie und Energetik kleiner Bleikristalle *Doctoral Thesis* RWTH Aachen, Germany
[27] Emundts A, Nowicki M and Bonzel H P 2002 *Surf. Sci.* **496** L35–42
[28] Arenhold K, Surnev S, Bonzel H P and Wynblatt P 1999 *Surf. Sci.* **424** 271
[29] Thürmer K, Reutt-Robey J E, Williams E D, Uwaha M, Emundts A and Bonzel H P 2001 *Phys. Rev. Lett.* **87** 186102
[30] Bombis C, Emundts A, Nowicki M and Bonzel H P 2002 *Surf. Sci.* **511** 83–96
[31] Kuipers L, Hoogeman M S and Frenken J W M 1993 *Phys. Rev. Lett.* **71** 3517
[32] Surnev S, Arenhold K, Coenen P, Voigtländer B, Bonzel H P and Wynblatt P 1998 *J. Vac. Sci. Technol.* A **16** 1059
[33] Mullins W W and Rohrer G S 2000 *J. Am. Ceram. Soc.* **83** 214
[34] Combe N, Jensen P and Pimpinelli A 2000 *Phys. Rev. Lett.* **85** 110
[35] Rohrer G S, Rohrer C L and Mullins W W 2001 *J. Am. Ceram. Soc.* **84** 2099–104
[36] Sáenz J J and García N 1985 *Surf. Sci.* **155** 24
[37] Williams E D, Phaneuf R J, Wei J, Bartelt N C and Einstein T L 1993 *Surf. Sci.* **294** 219
[38] Williams E D, Phaneuf R J, Wei J, Bartelt N C and Einstein T L 1994 *Surf. Sci.* **310** 451
[39] Akutsu Y, Akutsu N and Yamanoto T 1988 *Phys. Rev. Lett.* **61** 424
[40] Akutsu N and Akutsu Y 1999 *J. Phys.: Condens. Matter* **11** 6635
[41] Bonzel H P and Emundts A 2000 *Phys. Rev. Lett.* **84** 5804
[42] Mansfield M and Needs R J 1991 *Phys. Rev.* B **43** 8829
[43] Shilkrot L E and Srolovitz D J 1996 *Phys. Rev.* B **53** 11 120
[44] Wortis M 1988 *Chemistry and Physics of Solid Surfaces* vol 7, ed R Vanselow and R Howe (New York: Springer) pp 367–405
[45] Thürmer K, Reutt-Robey J E and Williams E D 2002 *Surf. Sci.* submitted